KONA Powder and Particle Journal

KONA Powder and Particle Journal No. 42 (2025) 188–199/https://doi.org/10.14356/kona.2025013 Review Paper

Perspectives on Particle Design Strategies for Better Inactivation of Airborne Pathogens †

Mohaiminul Haider Chowdhury $, Zan Zhu $ and Wei-Ning Wang *

College of Engineering, Virginia Commonwealth University, USA

Airborne pathogens such as bacteria, viruses and fungi pose significant threats to human health. Various mitigation strategies have been developed, including air filtration, ventilation, UV irradiation, and photocatalytic oxidative disinfection (POD). In particular, the combination of passive air filtration and active POD has promise for the better inactivation of airborne pathogens. However, the efficiency of POD remains hindered by numerous factors, such as inherent fast charge recombination, limited understanding of the interactions between airborne pathogens and catalyst surfaces, and short migration distances of reactive oxygen species (ROS). This perspective elucidates the fundamental principles and constraints of POD and provides several examples for delineating enhancement strategies. The primary objective of this study is to cultivate a cellular-level understanding of the interactions occurring at the biointerfaces in POD systems, thereby revealing the mechanistic pathways and paving the way for future catalyst designs to improve air quality.

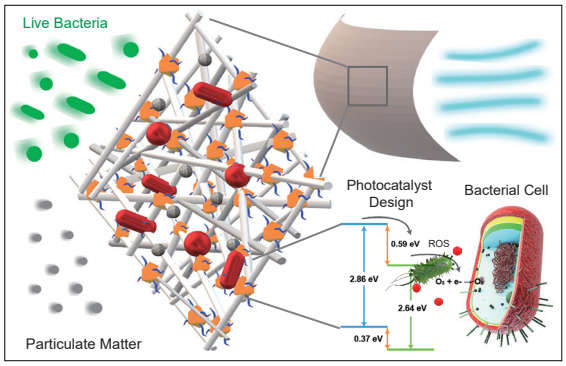

Keywords: air filtration, COVID, airborne pathogens, photocatalysis, disinfection

1. Introduction

The World Health Organization (WHO) reports that indoor air pollution causes 3.8 million deaths worldwide each year (Balmes, 2019). Indoor air quality, therefore, has increasingly become an alarming concern within the scientific community due to the growing health impacts such as cancer, asthma, and bronchitis, induced by poor air quality (Balakrishnan et al., 2014; Burnett et al., 2014). Indoor air pollutants include particulate matter (PM), volatile inorganic compounds (VIC), and volatile organic compounds (VOC) (Gonzalez-Martin et al., 2021). Of particular concern are airborne pathogens, which are a unique component of PM. They are clustered into three major groups: bacteria, fungi, and viruses (Song et al., 2022). Different airborne pathogens can cause a plethora of diseases, such as common colds, flu, asthma, anthrax, tuberculosis, botulism, and pneumonia (Bhardwaj et al., 2021; Xu Z.Q. et al., 2012) (see **Table 1**).

The recent COVID-19 pandemic was also caused by the airborne SARS-CoV-2 virus, which can spread through airborne transmission. This global health crisis underscored the critical importance of air biosecurity, as the transmission of the SARS-CoV-2 virus through respiratory droplets and aerosol particles emerged as the primary mode of spread (Guo et al., 2023; Vlaskin, 2022).

Over the years, strategies for controlling airborne pathogens have been developed and are generally classified based on two fundamental principles: capture and inactivation, as depicted in **Fig. 1**.

Among these strategies, air filtration using HVAC filters and face masks is the most viable tool to control air quality, protecting people from inhaling PM and airborne pathogens. However, although most commercial filters can capture airborne pathogens on their surfaces, they cannot inactivate them, posing a risk of secondary contamination under high airflow.

In particular, bio-contaminated surfaces in hospital buildings, equipment, and even personal protective equipment (PPE) are considered sources of secondary contamination, leading to hospital-acquired infections (HAI), also known as health-associated infections (Magill et al., 2014; Peleg and Hooper, 2010). Effective disinfection strategies are crucial to prevent these transmissions. Typically, harsh chemicals, e.g., chlorine dioxide and ethylene oxide are used, which, however, are often associated with several adverse effects (Hubbard et al., 2009). Ultraviolet (UV) sterilization by direct UV-C irradiation is also employed, but this involves severe occupational risks (Kühn et al., 2003; Walker and Ko, 2007). Among these control

† Received 29 May 2024; Accepted 17 June 2024
J-STAGE Advance published online 10 August 2024
$ Authors contributed equally to this publication
* Corresponding author: Wei-Ning Wang;
Add: 401 W. Main St., Richmond, Virginia 23284, USA
E-mail: wnwang@vcu.edu
TEL: +1-804-827-4306 FAX: +1-804-827-7030

Table 1 Airborne pathogens and associated health risks.

Species	Airborne pathogens (Microorganisms)	Health impacts
Bacteria (Gram-Negative)	*Escherichia coli*	Gastroenteritis; abdominal cramps; diarrhea; vomiting
	Pseudomonas fluorescens	Septicemia
	Legionella pneumophila	Pneumonia; pulmonary infections; influenza
Bacteria (Gram-Positive)	*Staphylococcus epidermidis*	Food poisoning
	Staphylococcus aureus	Septicemia; endocarditis; meningitis; osteomyelitis
	Micrococcus luteus	Endocarditis; meningitis
	Mycobacterium	Tuberculosis
Fungi	*Aspergillus versicolor*	Gastroenteritis; abdominal cramps; diarrhea; vomiting
	Aspergillus niger	Ear infections; sore throat; bronchitis; skin infections
	Penicillium citrinum	Renal tumors
	Penicillium spinulosum	Septicemia
Viruses	Measles virus	Measles
	NWS/G70C (H11N9)	Pneumonia; pulmonary infections; influenza
	Norovirus	Gastroenteritis; abdominal cramps; diarrhea; vomiting
	Adenovirus	Ear, respiratory tract, gastrointestinal, and liver infections
	Varicella-zoster virus	Chickenpox

Source: (Bhardwaj et al., 2021; Xu Z.Q. et al., 2012)

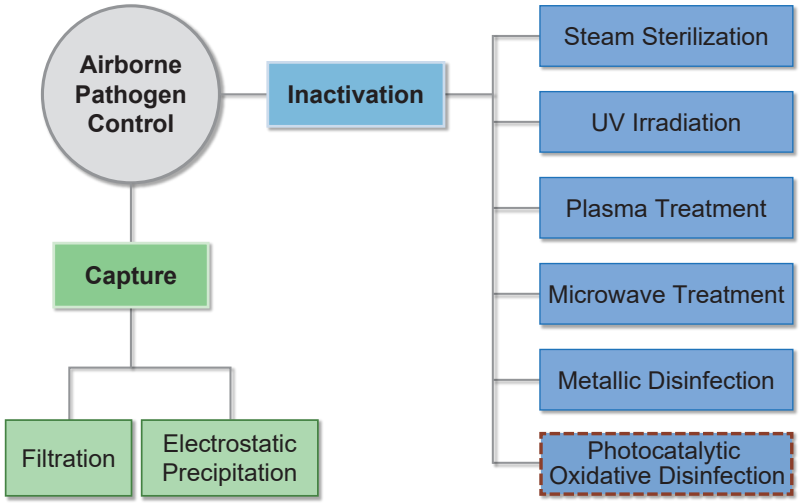

Fig. 1 Classification of various techniques for controlling airborne pathogens.

strategies, photocatalytic oxidative disinfection (POD) using catalyst particles has emerged as an efficient, cost-effective, environmentally sustainable approach (Hodges et al., 2018; Wang H.L. et al., 2014; Yu J.C. et al., 2005). Notably, combining passive air filtration and active POD may be a promising strategy for capturing airborne pathogens and simultaneously killing them *in situ*.

However, the POD efficiency remains low and is plagued by many factors, such as inherent fast charge recombination, limited understanding of the interactions between the captured pathogen cells and catalyst surface, and short migration distances (also times) of reactive oxygen species (ROS). The rational design of photocatalyst particles by addressing the constraints of the POD technique is thus essential.

In this perspective, we introduce the fundamental principles and constraints of the POD technique and provide several examples to delineate enhancement strategies. We used bacteria as the model airborne pathogens and metal-organic frameworks (MOFs) (Furukawa et al., 2013; Li P. et al., 2019) as supporting materials for efficient catalyst particle design. The primary objective of this study is

to cultivate a cellular-level understanding of the interactions occurring at the biointerfaces in POD systems, thereby revealing the mechanistic pathways and paving the way for future catalyst designs to improve air quality.

2. Principles and limitations of photocatalytic oxidative disinfection

Photocatalytic oxidative disinfection (POD) is a promising technology for killing airborne pathogens. In the POD system, the photocatalytic surface is activated by light to generate charge carriers, i.e., electron and hole pairs (**Fig. 2**) (Chen F.N. et al., 2010; Kim et al., 2021; Kumar et al., 2020; Li P. et al., 2019; Nosaka Y. and Nosaka A.Y., 2017; Shi et al., 2020; Wang W.J. et al., 2013).

Taking a water-based POD system as an example, these excited charge carriers react with water or oxygen molecules to form various reactive oxygen species (ROS), such as $\bullet O_2^-$, $^1O_2$, •OH, $\bullet O^-$, and $\bullet OO^-$ (Nosaka Y. and Nosaka A.Y., 2017). When a bacterial cell comes in contact with the photocatalytic surface through different forces such as electrostatic attraction, hydrophobic interactions, van der Waals forces, and receptor-ligand interactions, these ROS impact the bacterial cell membrane and also affect cell metabolism (Regmi et al., 2018). Consequently, these ROS damage bacterial cells, including the cell wall and intracellular components such as proteins, DNA, and lipids (**Fig. 3**) (Shi et al., 2020; You et al., 2019; Zeng et al., 2017). The proposed reactions for representative ROS formation and associated bacterial inactivation are described below (Regmi et al., 2018):

$$\text{Photocatalyst} + h\upsilon \rightarrow h^+ + e^-$$
$$h^+ + H_2O \rightarrow \bullet OH + H^+$$
$$h^+ + OH^- \rightarrow \bullet OH$$
$$e^- + O_2 \rightarrow \bullet O_2^- \xrightarrow{2H^+} H_2O_2 \xrightarrow{e^-} \bullet OH + OH^-$$
$$\bullet OH + \text{pathogen} + O_2 \rightarrow \text{simpler products (salts, } H_2O\text{, etc.)}$$

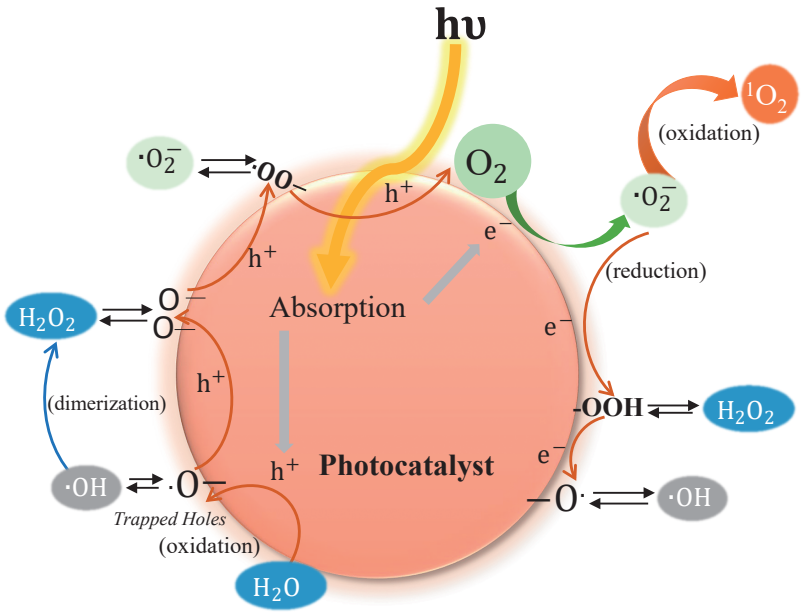

Fig. 2 Mechanism of ROS generation in the presence of light.

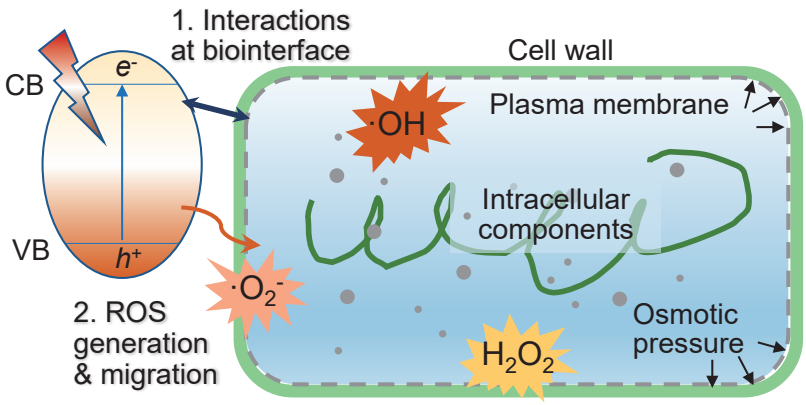

Fig. 3 Interactions between bacterial cells and photogenerated ROS at the biointerface.

Table 2 Half-life and migration distance of ROS.

ROS	Half-life time ($t_{1/2}$)	Migration distance
Superoxide ($\bullet O_2^-$)	1–4 μs	30 nm
Singlet Oxygen ($^1O_2$)	1–4 μs	30 nm
Hydroxyl radicals (•OH)	1 μs	1 nm
Hydrogen Peroxide (H_2O_2)	1 ms	1 μm

Despite being a promising antimicrobial strategy, the POD system is inefficient. The major challenge in this system is the rapid electron–hole (e^-–h^+) recombination, which typically occurs within nanoseconds, two or three orders of magnitude faster than other charge transfer processes (Fujishima et al., 2008; Hoffmann et al., 1995). Over the past decades, constant efforts have been made to address this critical issue and improve the overall POD efficiency by developing strategies such as incorporating metal sinks and creating heterojunctions (Ahmad et al., 2023; Linsebigler et al., 1995; Serpone and Emeline, 2012).

However, in a typical POD system, ROS are generated on the photocatalyst surface, typically with very short half-life times ($t_{1/2}$) and migration distances (see **Table 2**).

The short lifespans and migration distances of photogenerated ROS often result in their degradation into less potent species before they reach bacterial cells. Consequently, the efficacy of bacterial inactivation is heavily dependent on the overall ROS concentration in the system. For instance, despite being 100 times more potent than $\bullet O_2^-$ and H_2O_2, •OH does not achieve its full antimicrobial capability as it has a significantly shorter migration distance compared to others, which restricts overall bactericidal efficacy (Das and Roychoudhury, 2014; Kusiak-Nejman and Morawski, 2019; Nasir et al., 2021).

In addition, bacterial cells are rich in carboxylic and phosphate groups, rendering them negatively charged. This often results in electrical repulsion, preventing bacterial adhesion on the catalytic surface of most metal oxide-based photocatalysts, which are also negatively charged due to the presence of hydroxyl groups. In such scenarios, antimicrobial activity depends on ROS diffusion and penetration into the bacterial cells (Cho et al., 2004). Therefore, the distance between the bacterial cell and catalyst surface can be reduced to further enhance the POD efficiency.

3. Particle design strategies

In this perspective, we present specific particle design strategies to address the aforementioned limitations by using metal-organic frameworks (MOFs) and quaternary ammonium compounds (QAC) as model materials. As emerging porous polymers, MOFs exhibit exceptionally high surface areas, rich surface chemistry, and tunable porous structures, making them well-suited for a range of catalytic applications (Jiao et al., 2019; Li D. et al., 2024; Yusuf et al., 2022). Conversely, QAC compounds are widely known for their antibacterial properties due to factors such as low toxicity, structural flexibility, ease of surface fixation, and minimal risk of antibiotic resistance (Ping et al., 2019; Sun et al., 2020; Zander et al., 2018; Zhang et al., 2020). The N^+ in QAC electrostatically attracts negatively charged bacterial cells, which ultimately leads to cell lysis (Jennings et al., 2015; Wilson et al., 2001).

Based on these considerations, we implemented two strategies to develop MOF-based particles with QAC coatings, addressing the challenges of shorter ROS lifespan, shorter migration distance, and greater charge-carrier recombination. First, we developed a self-decontaminating nanofibrous filter (UiO-PQDMAEMA@PAN) for enhanced ROS interaction with bacterial cells (Zhu et al., 2021), where UiO refers to a zirconium-based MOF, PQDMAEMA refers to poly[2-(dimethyl decyl ammonium) ethyl methacrylate], and PAN indicates polyacrylonitrile. Second, we rationally designed heterojunction photocatalyst particles by modulating the surface of g-C_3N_4/MIL-125-NH_2 with a positive QAC layer (QAC@g-C_3N_4/MIL-125-NH_2) (Zhu et al., 2023). Here, g-C_3N_4 is a two-dimensional semiconductor, and MIL-125-NH_2 is a titanium-based MOF (Li P. et al., 2019; Ong et al., 2016; Zhou et al., 2020). This design aims to improve its affinity for bacterial cells and enhance electron–hole separation. The details of the design strategies and antimicrobial performance of the two materials are explained here.

3.1 UiO-PQDMAEMA@PAN filter

Synthesis of nanofibers. The entire synthesis route of the UiO-PQDMAEMA@PAN filter is schematically illustrated in **Figs. 4(a)** and **4(b)**. Initially, UiO-PQDMAEMA particles were prepared using UiO-66-NH_2 as the base material, which was then decorated with 2-bromoisobutyryl bromide (BIBB) to form UiO-66-BIBB. Next, using the atomic transfer radical polymerization (ATRP) method, the monomer 2-(dimethyl decyl ammonium) ethyl methacrylate (QDMAEMA) was polymerized and grafted onto the surface of UiO-66-BIBB to obtain UiO-PQDMAEMA.

The antibacterial nanofibrous filter was then fabricated through a facile electrospinning process by embedding UiO-PQDMAEMA particles in polyacrylonitrile (PAN) polymers. By varying parameters such as concentration, particle/polymer ratio, temperature, and relative humidity (RH), a range of nanofibers can be prepared.

Optimization of the nanofibers. In a typical electrospinning process, a well-mixed polymer solution of filler particles is generally used, resulting in a uniform distribution of filler particles within the polymer backbone in the final

nanofibers (Zhang et al., 2016). However, this homogenous structure is undesirable because it limits the catalytic performance of the embedded particles. To fully exploit the antimicrobial properties of UiO-PQDMAEMA, the particles must be exposed to the fiber surface.

To address this issue, an engineered strategy was implemented. The diameter of the PAN fiber backbone was optimized to be smaller than that of the UiO-PQDMAEMA particles ($d \cong 213$ nm). This optimization was based on understanding the fiber scaling law in electrospinning, where the equilibrium between the liquid's surface tension and the repellent electrostatic force determines the terminal fiber diameter (Schaate et al., 2011):

$$d_f \sim \left(\gamma \frac{Q^2}{I^2}\right)^{\frac{1}{3}} w_p^{\frac{1}{2}} \quad (1)$$

Here, Q is the feeding flowrate, I is the electric current in the system, w_p is the polymer volume fraction, and γ is the surface tension of the polymer solution, which can be expressed as follows (Xiao et al., 2017):

$$\gamma = \gamma^0 \left(1 - \frac{T}{T_c}\right)^n \quad (2)$$

where γ^0 is the constant of each liquid, n is a positive empirical factor, T_c is the critical temperature and T is the working temperature. According to **Eqn. (1)**, a decrease in γ will decrease the terminal fiber diameter. In this study, we rationally increased the working temperature of the polymer solution to reduce the surface tension while keeping Q, I, and w_p constant. The relative humidity (RH) was maintained as low as 10 % to facilitate the production of thinner fibers because a lower RH aids solvent evaporation (Xu J.W. et al., 2015). As shown in **Fig. 4(c)**, the pure PAN fibers have smooth surfaces and an average diameter of ~139 nm. The morphology of the UiO-PQDMAEMA@PAN filter was much rougher, with UiO-PQDAMEMA particles distributed on the fiber surface (**Fig. 4(d)**). This arrangement allows PQDMAEMA particles to come into direct contact with more bacterial cells.

Particle and Bacterial Filtration Tests. The experimental setup of the filtration tests is illustrated in **Fig. 5**. The particle filtration tests were conducted based on the international standard (ISO 21083-1, 2018) using monodispersed NaCl as model particles. The system includes an atomizer to generate NaCl particles, a Po^{210} neutralizer to achieve Boltzmann equilibrium during charging (Tang et al., 2018), a differential mobility analyzer (DMA, Model 3082, TSI Inc.) to select specific particle sizes, and a filter system

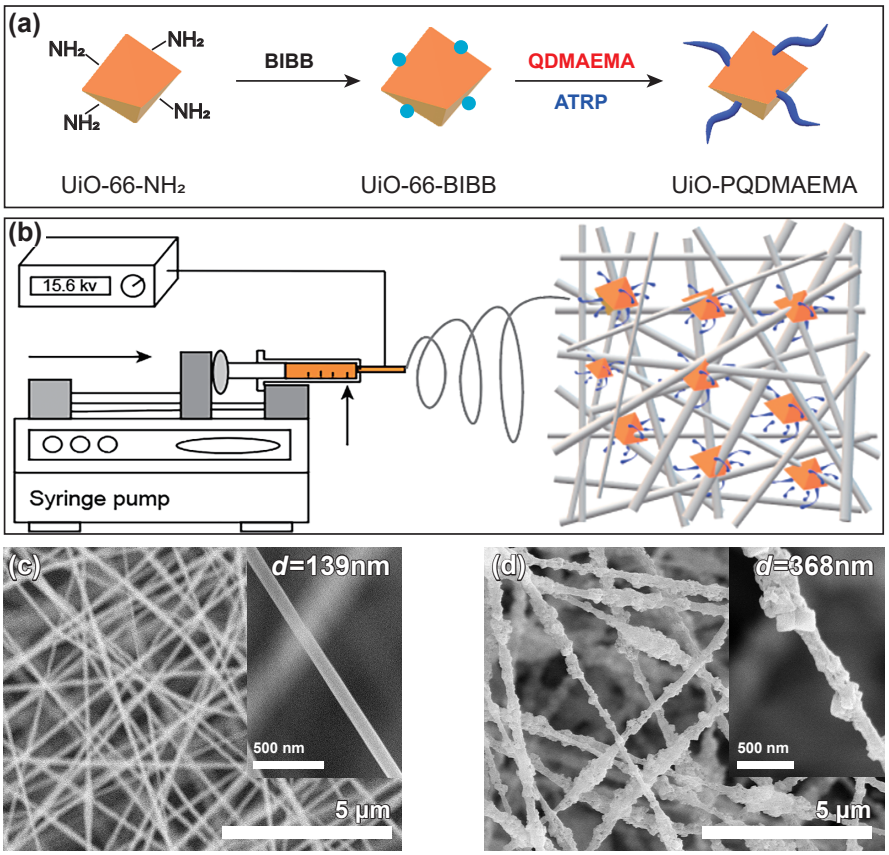

Fig. 4 **(a)** Synthesis route for UiO-PQDMAEMA from UiO-66-NH_2, **(b)** Schematic electrospinning process for nanofiber fabrication, **(c)** SEM image of pure PAN fibers, **(d)** SEM image of UiO-PQDMAEMA@PAN fibers. Reprinted with permission from Ref. (Zhu Z. et al., 2021). Copyright: (2021) The Royal Society of Chemistry.

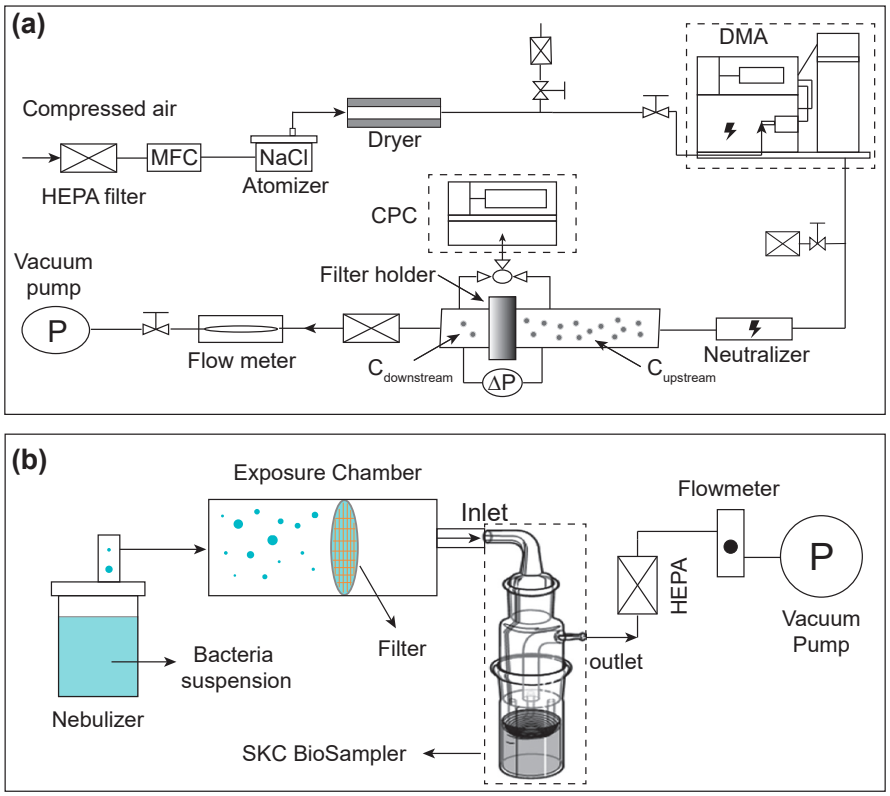

Fig. 5 Schematic diagram of experimental setup for **(a)** particle and **(b)** bacteria filtration tests. Reprinted with permission from Ref. (Zhu Z. et al., 2021). Copyright: (2021) The Royal Society of Chemistry.

(**Fig. 5(a)**). The particle filtration efficiency was calculated from **Eqn. (3)** using the upstream and downstream particle number concentrations measured using an ultrafine condensation particle counter (UCPC, Model 3776, TSI Inc.). The same calculation was performed using a commercial N95 respirator (VWR Makrite®) for comparison.

$$PFE\,(\%) = \left(1 - \frac{C_{\text{downstream}}}{C_{\text{upstream}}}\right) \times 100\% \tag{3}$$

Filtration tests for *S. epidermidis* (Gram-positive) and *E. coli* (Gram-negative) bacteria were conducted as shown in **Fig. 5(b)**. The bacteria cells were first suspended in phosphate-buffered saline (PBS) solution at a density of 10^7 CFU/mL. An ultrasonic nebulizer (2.4 MHz) was used to atomize the suspension. The generated bioaerosols were bombarded onto the filter surface at a flow rate of 12.5 L/min for 1 min. The escaped bioaerosols were collected in a sterile PBS solution using a BioSampler (SKC Inc.). **Eqn. (4)** defines the bacterial filtration efficiency (*BFE*) of the filter.

$$BFE = \left[\left(1 - \frac{C_{\text{f}}}{C_{\text{total}}}\right)\right] \times 100\% \tag{4}$$

where C_{f} and C_{total} are the bacteria concentrations in the BioSampler with and without a filter, respectively.

As shown in **Fig. 6(a)**, the particle filtration efficiency decreased until it approached the most penetrating particle size (MPPS), which was approximately 80 nm. The efficiency of the UiO-PQDMAEMA@PAN filter in measuring 80 nm PM was found to be ~95.4 %, which is comparable to the conventional N95 respirator standard in terms of PM filtration.

The hierarchical structures within the electrospun fibers of the UiO-PQDMAEMA@PAN filter likely contributed to its superior filtering performance when tested under the same pressure drop (52.3 Pa) as pure PAN filters (Chang et al., 2016), where more active sites for interaction between particles and composite electrospun fibers are available (Chen S.C. et al., 2014).

Another crucial parameter of mask filters is the pressure drop (ΔP), which affects user comfort. The quality factor (QF) is used to measure the pressure drop performance of a filter, which is defined as follows:

$$QF = \frac{\ln(1 - PFE)}{\Delta P} \tag{5}$$

As shown in **Fig. 6(b)**, the UiO-PQDMAEMA@PAN fibers exhibit satisfactory *QFs* that are substantially better than those of pure PAN fibers. The minimal QF value of 0.058 at an MPPS of 80 nm for the UiO-PQDMAEMA@PAN filter indicates again that its peak filtration performance is comparable to that of commercial N95 respirators (0.056).

In contrast to the particle filtration results, all atomized

bacterial cells were captured using a UiO-PQDMAEMA@PAN filter and a commercial N95 respirator (Zhu et al., 2021). This is expected because bacterial cells typically have sizes in the range of 0.5 to 2 μm, which is much larger than the MPPS of the filter, i.e., 80 nm, as discussed above.

Bactericidal Evaluation. In addition to filtration measurements, bacterial inactivation experiments were conducted. As shown in **Figs. 6(c)** and **6(d)**, the UiO-PQDMAEMA filters outperformed all other control filters, achieving an inactivation efficiency of ~97.4 % for *S. epidermidis* and ~95.1 % for *E. coli*. This indicates that the grafted UiO-PQDMAEMA on the surface of the PAN fibers allows the filter to exhibit efficient bactericidal behavior. Numerous contacting sites of positively charged UiO-PQDMAEMA (N^+) are responsible for capturing and killing bacterial cells *in situ* by lysing their cytoplasm (Gozzelino et al., 2013).

3.2 QAC@ g-C_3N_4/MIL-125-NH_2 particles

Synthesis of photocatalysts. The heterojunction QAC@*g*-C_3N_4/MIL-125-NH_2 (C-M-Q) photocatalyst particles were synthesized in several steps, as shown in **Fig. 7**.

The bare catalyst particles *g*-C_3N_4/MIL-125-NH_2 (C-M) were first synthesized by a solvothermal method in which pre-synthesized *g*-C_3N_4 was suspended in the MIL-125-NH_2 precursor. The mixture was then heated in a Teflon-lined steel autoclave at 150 °C for 15 h (Wang H. et al., 2015). The C-M particles were then coated with QAC, where the QDMAEMA monomer was polymerized and grafted on the surface of C-M through ATRP (Hippeli and Elstner, 1997) to obtain QAC@*g*-C_3N_4/MIL-125 (C-M-Q) particles.

Photocatalytic performance. Synthesizing heterojunction semiconductor catalysts with proper band gap alignment is a promising approach to mitigate rapid charge recombination, i.e., better e^-–h^+ separation to enhance photocatalytic performance (Hippeli and Elstner, 1997).

The band alignment between *g*-C_3N_4 and MIL-125-NH_2 was determined following the Kraut method (Kraut et al., 1980; Zhao et al., 2019) using X-ray photoelectron spectroscopy (XPS) and UV-Vis spectroscopy. As illustrated in **Fig. 8(a)**, the enhanced charge transfer within the heterojunction was achieved.

Bacterial inactivation experiments were conducted in PBS solution under visible light irradiation with *S. epidermidis*, which was selected as the representative bacterium for the POD tests. As shown in **Fig. 8(b)**, the bare photocatalyst C-M exhibited an unnoticeable reduction of bacterial cells in the dark, whereas under light irradiation, it achieved a 1.5 log reduction, suggesting that the

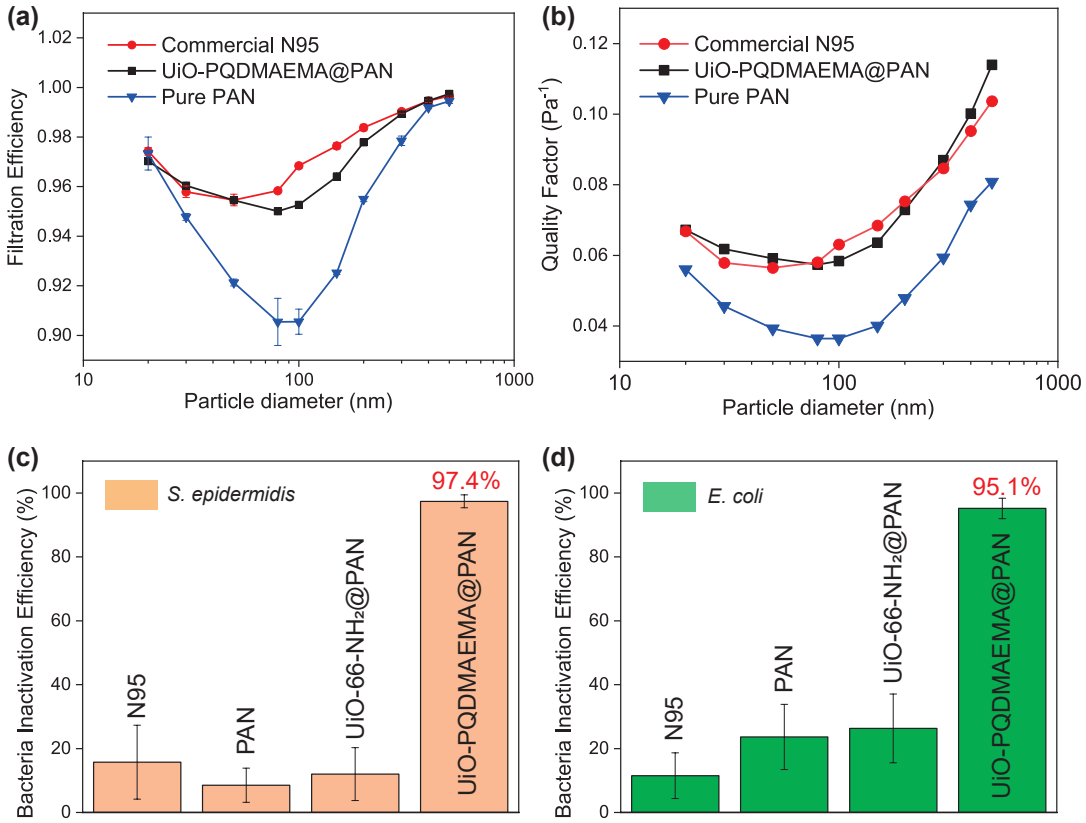

Fig. 6 **(a)** Particle filtration efficiency and **(b)** quality factor of different filters tested using NaCl particles of 20–500 nm at a face velocity of 9.3 cm/s; the inactivation performance of different filters toward **(c)** *S. epidermidis* and **(d)** *E. coli*. Reprinted with permission from Ref. (Zhu Z. et al., 2021). Copyright: (2021) The Royal Society of Chemistry.

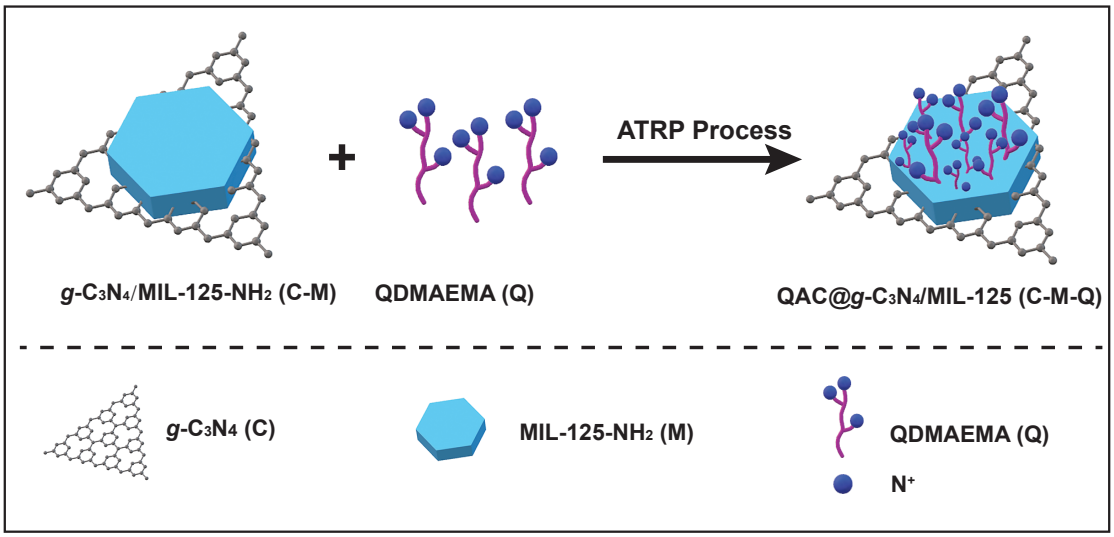

Fig. 7 Synthesis of QAC@g-C_3N_4/MIL-125 (C-M-Q) particles. Reprinted with permission from Ref. (Zhu Z. et al., 2023). Copyright: (2023) Elsevier.

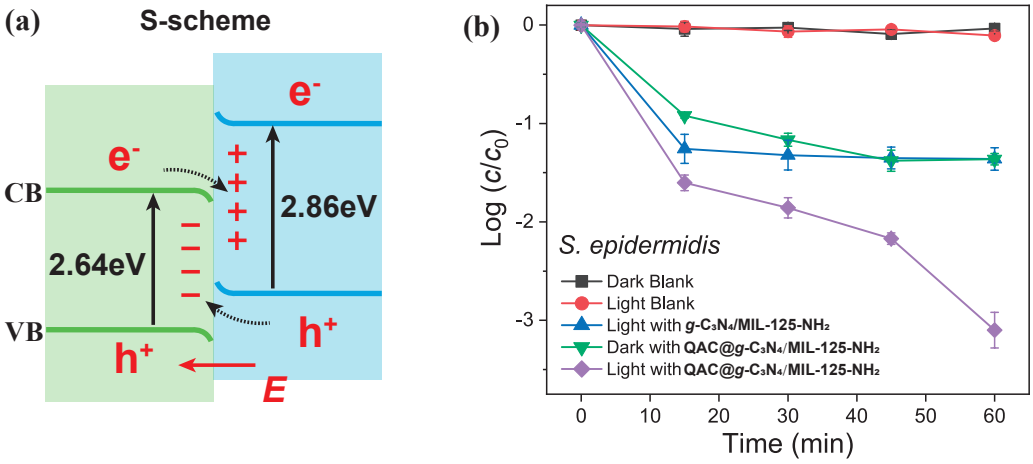

Fig. 8 **(a)** Schematic illustration of band alignment and charge transfer in C-M-Q and **(b)** time course of the bactericidal activities of C-M-Q in *S. epidermidis* under different conditions. Reprinted with permission from Ref. (Zhu Z. et al., 2023). Copyright: (2023) Elsevier.

bactericidal activity was mainly due to the photogenerated ROS in the solution rather than the toxicity of the catalyst itself. Interestingly, C-M-Q achieved a 1.54 log reduction of *S. epidermis* in the dark via the contact killing mechanism due to the QAC coating (Kaur and Liu, 2016). When light was applied, a significantly enhanced bactericidal efficiency (3.2 log reduction) was obtained. Therefore, at the biointerface, the photogenerated ROS and the positively charged QAC layer exhibit cooperative antibacterial behavior, which significantly improves the overall bactericidal activity.

Visualization and quantification of bacteria-photocatalyst interactions. To further understand the interactions between *S. epidermidis* cells and the C-M-Q surface, the direct visualization and quantification of these interactions at the biointerface were conducted via atomic force microscopy (AFM) using the peak force quantitative nano-mechanical (QNM) mode. As shown in **Fig. 9(a)**, these measurements were performed in PBS solution (pH 7.4) to avoid potential errors due to capillary forces that arose from the humid coverage of both the sample and the AFM tip under ambient conditions (Asri et al., 2014; Hoogenboom et al., 2008).

Specifically, the AFM probe was first functionalized with the C-M-Q particles (**Figs. 9(b)** and **9(c)**), which were then used to measure the adhesion forces. **Figs. 9(d)–9(f)** display the peak force error image, adhesion map, and force curve of S. *epidermidis* cells using the pristine AFM probe as the control. The same results were obtained for the C-M-Q-functionalized probe (**Figs. 9(g)–9(i)**).

As seen from the measurement results, in comparison with the bare probe in the approach curve, the attractive electrostatic effects in C-M-Q were noticed much earlier due to the presence of a positively charged QAC layer. Additionally, a significantly higher adhesion force (F_{adh}) of 972 pN was found between C-M-Q and the bacterial cells

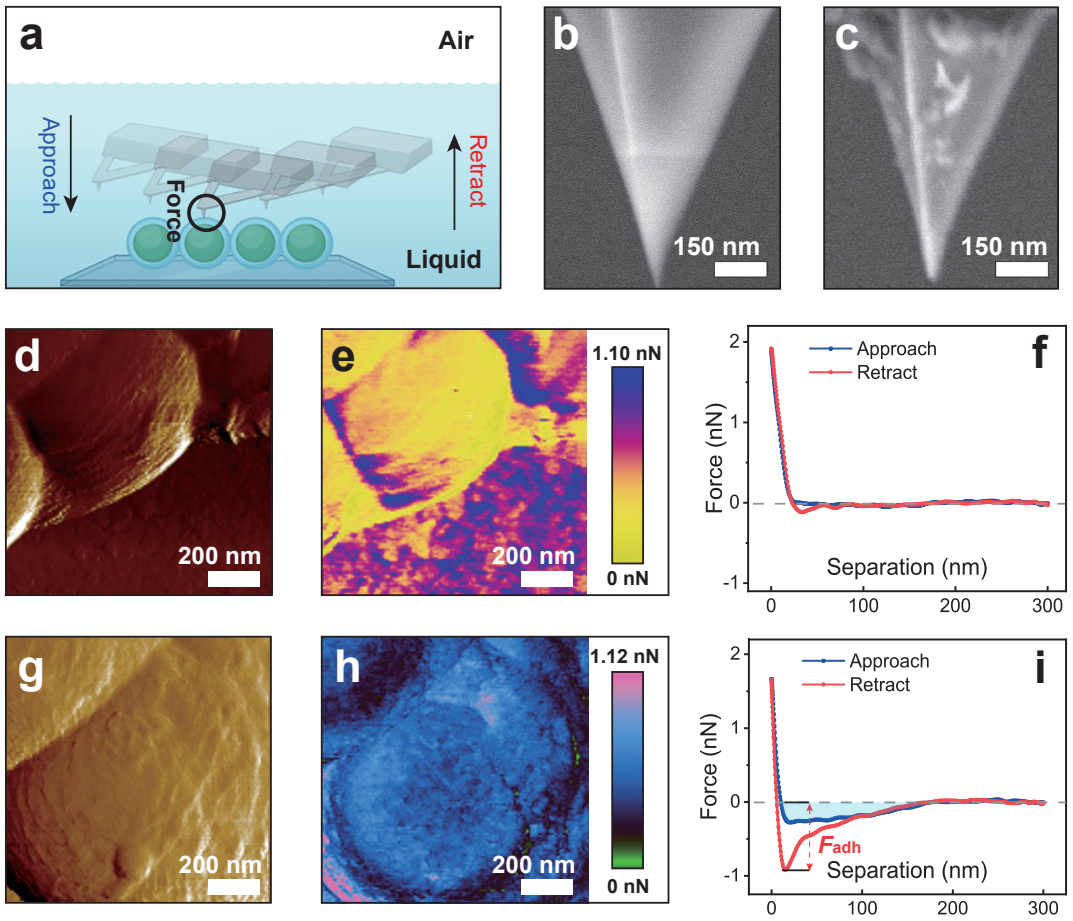

Fig. 9 AFM measurements of interactions between *S. epidermidis* cells and the C-M-Q photocatalyst. **(a)** Illustration of the AFM force measurement in PBS solution; SEM images of **(b)** the pristine AFM probe and **(c)** the C-M-Q coated probe; **(d,e,f)** and **(g,h,i)** show the peak force error image, adhesion force mapping, and approach-retract force curves of *S. epidermidis* cells measured using the pristine AFM probe and the photocatalyst-coated probe, respectively. Reprinted with permission from Ref. (Zhu Z. et al., 2023). Copyright: (2023) Elsevier.

(**Fig. 9(i)**), whereas only 115 pN was detected between the unmodified probe and the bacterial cells (**Fig. 9(f)**). The results reflect that the positive charge modulation of the photocatalyst surface facilitates bacterial adhesion, which in turn enhances the overall bactericidal performance.

4. Conclusions and perspectives

This perspective introduces the fundamental principles of POD and its enhancement strategies by providing several examples. We rationally designed and fabricated several novel antimicrobial MOF-based particles to effectively kill airborne bacterial cells. Specifically, QAC polymer, a broad-spectrum antimicrobial agent, was carefully coated on the surface of MOF-based particles to form active composites capable of attracting and killing bacterial cells *in situ*. These composite particles exhibit excellent antibacterial activity, with contact killing and photogenerated ROS responsible for efficient disinfection. The results also show that the adhesion of bacterial cells to the catalyst surface significantly enhances the photocatalytic bactericidal efficiency.

In addition, several perspectives are provided to further advance the POD technique for combating airborne pathogens as follows:

1) Understanding the mechanistic pathways of POD is crucial for designing photocatalyst particles. In particular, quantifying the characteristic times and migration distances of ROS and other intermediates along with their oxidative capacity in the system should be considered carefully.
2) The interactions between photocatalysts and pathogen cells should also be quantified at the molecular or atomic level using advanced *in situ* techniques, such as AFM and/or TEM.
3) Achieving multifunctional MOF-based materials to mitigate air pollution is promising but challenging. For example, coating polymers around MOF materials reduces specific surface areas and blocks active sites, adversely affecting gas adsorption. Therefore, “trade-off” effects should be seriously considered in material design.
4) Last but not least, the results obtained for bacterial

inactivation may not be easily applied to other airborne pathogens, such as viruses and fungi. Additional work is required in this regard.

Acknowledgments

This work was supported by the National Science Foundation (CMMI-1727553), the Center for Innovative Technology (CIT) through the Virginia Commonwealth Research Commercialization Fund (CRCF) program, and the COVID-19 Rapid Research Funding Program at Virginia Commonwealth University (VCU). The authors thank Dr. Ping Xu from the VCU School of Dentistry and Dr. Shawn Chen from the VCU College of Engineering for their collaborations on this project. This perspective is based on Dr. Zan Zhu's Ph.D. dissertation entitled "Rational Design of Metal-Organic Frameworks (MOFs)-based Functional Materials Toward Better Air Quality."

References

Ahmad I., Zou Y., Yan J., Liu Y., Shukrullah S., Naz M.Y., Hussain H., Khan W.Q., Khalid N.R., Semiconductor photocatalysts: a critical review highlighting the various strategies to boost the photocatalytic performances for diverse applications, Advances in Colloid and Interface Science, 311 (2023) 102830. https://doi.org/10.1016/j.cis.2022.102830

Asri L.A.T.W., Crismaru M., Roest S., Chen Y., Ivashenko O., Rudolf P., Tiller J.C., van der Mei H.C., Loontjens T.J.A., Busscher H.J., A shape-adaptive, antibacterial-coating of immobilized quaternary-ammonium compounds tethered on hyperbranched polyurea and its mechanism of action, Advanced Functional Materials, 24 (2014) 346–355. https://doi.org/10.1002/adfm.201301686

Balakrishnan K., Ghosh S., Ganguli B., Sambandam S., Bruce N.G., Barnes D.F., Erratum: "An integrated risk function for estimating the global burden of disease attributable to ambient fine particulate matter exposure", Environmental Health Perspectives, 122 (2014) A235. https://doi.org/10.1289/ehp.122-A235

Balmes J.R., Household air pollution from domestic combustion of solid fuels and health, Journal of Allergy and Clinical Immunology, 143 (2019) 1979–1987. https://doi.org/10.1016/j.jaci.2019.04.016

Bhardwaj S.K., Bhardwaj N., Kumar V., Bhatt D., Azzouz A., Bhaumik J., Kim K.H., Deep A., Recent progress in nanomaterial-based sensing of airborne viral and bacterial pathogens, Environment International, 146 (2021) 106183. https://doi.org/10.1016/j.envint.2020.106183

Burnett R.T., Pope C.A., Ezzati M., Olives C., Lim S.S., Mehta S., Shin H.H., Singh G., Hubbell B., Brauer M., Anderson H.R., Smith K.R., Balmes J.R., Bruce N.G., Kan H., et al., An integrated risk function for estimating the global burden of disease attributable to ambient fine particulate matter exposure, Environmental Health Perspectives, 122 (2014) 397–403. https://doi.org/10.1289/ehp.1307049

Chang D.Q., Chen S.C., Pui D.Y.H., Capture of sub-500 nm particles using residential electret HVAC filter media-experiments and modeling, Aerosol and Air Quality Research, 16 (2016) 3349–3357. https://doi.org/10.4209/aaqr.2016.10.0437

Chen F.N., Yang X.D., Mak H.K.C., Chan D.W.T., Photocatalytic oxidation for antimicrobial control in built environment: a brief literature overview, Building and Environment, 45 (2010) 1747–1754. https://doi.org/10.1016/j.buildenv.2010.01.024

Chen S.C., Wang J., Bahk Y.K., Fissan H., Pui D.Y.H., Carbon nanotube penetration through fiberglass and electret respirator filter and Nuclepore filter media: experiments and models, Aerosol Science and Technology, 48 (2014) 997–1008. https://doi.org/10.1080/02786826.2014.954028

Cho M., Chung H., Choi W., Yoon J., Linear correlation between inactivation of *E. coli* and OH radical concentration in TiO_2 photocatalytic disinfection, Water Research, 38 (2004) 1069–1077. https://doi.org/10.1016/j.watres.2003.10.029

Das K., Roychoudhury A., Reactive oxygen species (ROS) and response of antioxidants as ROS-scavengers during environmental stress in plants, Frontiers in Environmental Science, 2 (2014) 53. https://doi.org/10.3389/fenvs.2014.00053

Fujishima A., Zhang X.T., Tryk D.A., TiO_2 photocatalysis and related surface phenomena, Surface Science Reports, 63 (2008) 515–582. https://doi.org/10.1016/j.surfrep.2008.10.001

Furukawa H., Cordova K.E., O'Keeffe M., Yaghi O.M., The chemistry and applications of metal-organic frameworks, Science, 341 (2013) 1230444. https://doi.org/10.1126/science.1230444

Gonzalez-Martin J., Kraakman N.J.R., Perez C., Lebrero R., Munoz R., A state-of-the-art review on indoor air pollution and strategies for indoor air pollution control, Chemosphere, 262 (2021) 128376. https://doi.org/10.1016/j.chemosphere.2020.128376

Gozzelino G., Lisanti C., Beneventi S., Quaternary ammonium monomers for UV crosslinked antibacterial surfaces, Colloid Surface A, 430 (2013) 21–28. https://doi.org/10.1016/j.colsurfa.2013.03.061

Guo L., Zhao P.Y., Jia Y.K., Wang Z.F., Chen M., Zhang H., Liu D.X., Zhang Y., Wang X.H., Rong M.Z., Inactivation of airborne pathogenic microorganisms by plasma-activated nebulized mist, Journal of Hazardous Materials, 459 (2023) 132072. https://doi.org/10.1016/j.jhazmat.2023.132072

Hippeli S., Elstner E.F., OH-radical-type reactive oxygen species: a short review on the mechanisms of OH-radical-and peroxynitrite toxicity, Zeitschrift für Naturforschung C, 52 (1997) 555–563. https://doi.org/10.1515/znc-1997-9-1001

Hodges B.C., Cates E.L., Kim J.H., Challenges and prospects of advanced oxidation water treatment processes using catalytic nanomaterials, Nature Nanotechnology, 13 (2018) 642–650. https://doi.org/10.1038/s41565-018-0216-x

Hoffmann M.R., Martin S.T., Choi W.Y., Bahnemann D.W., Environmental applications of semiconductor photocatalysis, Chemical Reviews, 95 (1995) 69–96. https://doi.org/10.1021/cr00033a004

Hoogenboom B.W., Frederix P.L.T.M., Fotiadis D., Hug H.J., Engel A., Potential of interferometric cantilever detection and its application for SFM/AFM in liquids, Nanotechnology, 19 (2008) 384019. https://doi.org/10.1088/0957-4484/19/38/384019

Hubbard H., Poppendieck D., Corsi R.L., Chlorine dioxide reactions with indoor materials during building disinfection: surface uptake, Environmental Science & Technology, 43 (2009) 1329–1335. https://doi.org/10.1021/es801930c

ISO 21083-1,Test method to measure the efficiency of air filtration media against spherical nanomaterials, Part 1: Size range from 20 nm to 500 nm, ISO (International Organization for Standardization), (2018). <https://www.iso.org/standard/69876.html> accessed 25072024.

Jennings M.C., Minbiole K.P.C., Wuest W.M., Quaternary ammonium compounds: an antimicrobial mainstay and platform for innovation to address bacterial resistance, ACS Infectious Diseases, 1 (2015) 288–303. https://doi.org/10.1021/acsinfecdis.5b00047

Jiao L., Seow J.Y.R., Skinner W.S., Wang Z.U., Jiang H.-L., Metal–organic frameworks: structures and functional applications, Materials Today, 27 (2019) 43–68. https://doi.org/10.1016/j.mattod.2018.10.038

Kaur R., Liu S., Antibacterial surface design – Contact kill, Progress in Surface Science, 91 (2016) 136–153. https://doi.org/10.1016/j.progsurf.2016.09.001

Kim Y., Coy E., Kim H., Mrowczynski R., Torruella P., Jeong D.W., Choi K.S., Jang J.H., Song M.Y., Jang D.J., Peiro F., Jurga S., Kim H.J., Efficient photocatalytic production of hydrogen by exploiting the polydopamine-semiconductor interface, Applied Catalysis B-Environmental, 280 (2021) 119423. https://doi.org/10.1016/j.apcatb.2020.119423

Kraut E.A., Grant R.W., Waldrop J.R., Kowalczyk S.P., Precise determination of the valence-band edge in X-ray photoemission spectra—application to measurement of semiconductor interface potentials, Physical Review Letters, 44 (1980) 1620–1623. https://doi.org/10.1103/PhysRevLett.44.1620

Kühn K.P., Chaberny I.F., Massholder K., Stickler M., Benz V.W., Sonntag H.G., Erdinger L., Disinfection of surfaces by photocatalytic oxidation with titanium dioxide and UVA light, Chemosphere, 53 (2003) 71–77. https://doi.org/10.1016/S0045-6535(03)00362-X

Kumar A., Raizada P., Singh P., Saini R.V., Saini A.K., Hosseini-Bandegharaei A., Perspective and status of polymeric graphitic carbon nitride based Z-scheme photocatalytic systems for sustainable photocatalytic water purification, Chemical Engineering Journal, 391 (2020) 123496. https://doi.org/10.1016/j.cej.2019.123496

Kusiak-Nejman E., Morawski A.W., TiO_2/graphene-based nanocomposites for water treatment: a brief overview of charge carrier transfer, antimicrobial and photocatalytic performance, Applied Catalysis B-Environmental, 253 (2019) 179–186. https://doi.org/10.1016/j.apcatb.2019.04.055

Li D., Yadav A., Zhou H., Roy K., Thanasekaran P., Lee C., Advances and applications of metal-organic frameworks (MOFs) in emerging technologies: a comprehensive review, Global Challenges, 8 (2024) 2300244. https://doi.org/10.1002/gch2.202300244

Li P., Li J.Z., Feng X., Li J., Hao Y.C., Zhang J.W., Wang H., Yin A.X., Zhou J.W., Ma X.J., Wang B., Metal-organic frameworks with photocatalytic bactericidal activity for integrated air cleaning, Nature Communications, 10 (2019) 2177. https://doi.org/10.1038/s41467-019-10218-9

Linsebigler A.L., Lu G.Q., Yates J.T., Photocatalysis on TiO_2 Surfaces - principles, mechanisms, and selected results, Chemical Reviews, 95 (1995) 735–758. https://doi.org/10.1021/cr00035a013

Magill S.S., Edwards J.R., Bamberg W., Beldavs Z.G., Dumyati G., Kainer M.A., Lynfield R., Maloney M., McAllister-Hollod L., Nadle J., Ray S.M., Thompson D.L., Wilson L.E., Fridkin S.K., Multistate point-prevalence survey of health care–associated infections, New England Journal of Medicine, 370 (2014) 1198–1208. https://doi.org/10.1056/NEJMoa1306801

Magill S.S., O'Leary E., Janelle S.J., Thompson D.L., Dumyati G., Nadle J., Wilson L.E., Kainer M.A., Lynfield R., Greissman S., Ray S.M., Beldavs Z., Gross C., Bamberg W., Sievers M., et al., Changes in prevalence of health care–associated infections in U.S. hospitals, New England Journal of Medicine, 379 (2018) 1732–1744. https://doi.org/10.1056/NEJMoa1801550

Nasir A.M., Awang N., Hubadillah S.K., Jaafar J., Othman M.H.D., Salleh W.N.W., Ismail A.F., A review on the potential of photocatalysis in combatting SARS-CoV-2 in wastewater, Journal of Water Process Engineering, 42 (2021) 102111. https://doi.org/10.1016/j.jwpe.2021.102111

Nosaka Y., Nosaka A.Y., Generation and detection of reactive oxygen species in photocatalysis, Chemical Reviews, 117 (2017) 11302–11336. https://doi.org/10.1021/acs.chemrev.7b00161

Ong W.J., Tan L.L., Ng Y.H., Yong S.T., Chai S.P., Graphitic carbon nitride ($g\text{-}C_3N_4$)-based photocatalysts for artificial photosynthesis and environmental remediation: are we a step closer to achieving sustainability?, Chemical Reviews, 116 (2016) 7159–7329. https://doi.org/10.1021/acs.chemrev.6b00075

Peleg A.Y., Hooper D.C., Hospital-acquired infections due to Gram-negative bacteria, New England Journal of Medicine, 362 (2010) 1804–1813. https://doi.org/10.1056/nejmra0904124

Ping M., Zhang X.R., Liu M.X., Wu Z.C., Wang Z.W., Surface modification of polyvinylidene fluoride membrane by atom-transfer radical-polymerization of quaternary ammonium compound for mitigating biofouling, Journal of Membrane Science, 570 (2019) 286–293. https://doi.org/10.1016/j.memsci.2018.10.070

Regmi C., Joshi B., Ray S.K., Gyawali G., Pandey R.P., Understanding mechanism of photocatalytic microbial decontamination of environmental wastewater, Frontiers in Chemistry, 6 (2018) 33. https://doi.org/10.3389/fchem.2018.00033

Schaate A., Roy P., Godt A., Lippke J., Waltz F., Wiebcke M., Behrens P., Modulated synthesis of Zr-based metal-organic frameworks: from nano to single crystals, Chemistry – A European Journal, 17 (2011) 6643–6651. https://doi.org/10.1002/chem.201003211

Serpone N., Emeline A.V., Semiconductor photocatalysis - past, present, and future outlook, The Journal of Physical Chemistry Letters, 3 (2012) 673–677. https://doi.org/10.1021/jz300071j

Shi H.X., Fan J., Zhao Y.Y., Hu X.Y., Zhang X., Tang Z.S., Visible light driven $CuBi_2O_4/Bi_2MoO_6$ p-n heterojunction with enhanced photocatalytic inactivation of *E. coli* and mechanism insight, Journal of Hazardous Materials, 381 (2020) 121006. https://doi.org/10.1016/j.jhazmat.2019.121006

Song L., Zhou J.F., Wang C., Meng G., Li Y.F., Jarin M., Wu Z.Y., Xie X., Airborne pathogenic microorganisms and air cleaning technology development: A review, Journal of Hazardous Materials, 424 (2022) 127429. https://doi.org/10.1016/j.jhazmat.2021.127429

Sun H.G., Du Y.W., Gao C.F., Iftikhar, Long J., Li S.W., Shao L., Pressure-assisted in-depth hydrophilic tailoring of porous membranes achieving high water permeability, excellent fouling resistance and superior antimicrobial ability, Journal of Membrane Science, 604 (2020) 118071. https://doi.org/10.1016/j.memsci.2020.118071

Tang M., Thompson D., Chen S.C., Liang Y., Pui D.Y.H., Evaluation of different discharging methods on HVAC electret filter media, Building and Environment, 141 (2018) 206–214. https://doi.org/10.1016/j.buildenv.2018.05.048

Vlaskin M.S., Review of air disinfection approaches and proposal for thermal inactivation of airborne viruses as a life-style and an instrument to fight pandemics, Applied Thermal Engineering, 202 (2022) 117855. https://doi.org/10.1016/j.applthermaleng.2021.117855

Walker C.M., Ko G., Effect of ultraviolet germicidal irradiation on viral aerosols, Environmental Science & Technology, 41 (2007) 5460–5465. https://doi.org/10.1021/es070056u

Wang H., Yuan X.Z., Wu Y., Zeng G.M., Chen X.H., Leng L.J., Li H., Synthesis and applications of novel graphitic carbon nitride/metal-organic frameworks mesoporous photocatalyst for dyes removal, Applied Catalysis B-Environmental, 174 (2015) 445–454. https://doi.org/10.1016/j.apcatb.2015.03.037

Wang H.L., Zhang L.S., Chen Z.G., Hu J.Q., Li S.J., Wang Z.H., Liu J.S., Wang X.C., Semiconductor heterojunction photocatalysts: design, construction, and photocatalytic performances, Chemical Society Reviews, 43 (2014) 5234–5244. https://doi.org/10.1039/c4cs00126e

Wang W.J., Yu J.C., Xia D.H., Wong P.K., Li Y.C., Graphene and $g\text{-}C_3N_4$ nanosheets cowrapped elemental α-sulfur as a novel metal-free heterojunction photocatalyst for bacterial inactivation under visible-light, Environmental Science & Technology, 47 (2013) 8724–8732. https://doi.org/10.1021/es4013504

Wilson W.W., Wade M.M., Holman S.C., Champlin F.R., Status of methods for assessing bacterial cell surface charge properties based on zeta potential measurements, Journal of Microbiological Methods, 43 (2001) 153–164. https://doi.org/10.1016/S0167-7012(00)00224-4

Xiao Q., Liang Y., Zhu F.W., Lu S.Y., Huang S., Microwave-assisted one-pot synthesis of highly luminescent N-doped carbon dots for cellular imaging and multi-ion probing, Microchimica Acta, 184 (2017) 2429–2438. https://doi.org/10.1007/s00604-017-2242-z

Xu J.W., Wang Y., Yang Y.F., Ye X.Y., Yao K., Ji J., Xu Z.K., Effects of quaternization on the morphological stability and antibacterial activity of electrospun poly(DMAEMA-co-AMA) nanofibers, Colloid Surface B, 133 (2015) 148–155. https://doi.org/10.1016/j.colsurfb.2015.06.002

Xu Z.Q., Shen F.X., Li X.G., Wu Y., Chen Q., Jie X., Yao M.S., Molecular and microscopic analysis of bacteria and viruses in exhaled breath collected using a simple impaction and condensing method, PLOS One, 7 (2012) e41137. https://doi.org/10.1371/journal.pone.0041137

You J.H., Guo Y.Z., Guo R., Liu X.W., A review of visible light-active photocatalysts for water disinfection: features and prospects, Chemical Engineering Journal, 373 (2019) 624–641. https://doi.org/10.1016/j.cej.2019.05.071

Yu J.C., Ho W.K., Yu J.G., Yip H., Wong P.K., Zhao J.C., Efficient visible-light-induced photocatalytic disinfection on sulfur-doped nanocrystalline titania, Environmental Science & Technology, 39 (2005) 1175–1179. https://doi.org/10.1021/es035374h

Yusuf V.F., Malek N.I., Kailasa S.K., Review on metal-organic framework classification, synthetic approaches, and influencing factors: applications in energy, drug delivery, and wastewater treatment, ACS Omega, 7 (2022) 44507–44531. https://doi.org/10.1021/acsomega.2c05310

Zander Z.K., Chen P.R., Hsu Y.H., Dreger N.Z., Savariau L., Mcroy W.C., Cerchiari A.E., Chambers S.D., Barton H.A., Becker M.L., Post-fabrication QAC-functionalized thermoplastic polyurethane for contact-killing catheter applications, Biomaterials, 178 (2018) 339–350. https://doi.org/10.1016/j.biomaterials.2018.05.010

Zeng X.K., Wang Z.Y., Meng N., McCarthy D.T., Deletic A., Pan J.H., Zhang X.W., Highly dispersed TiO_2 nanocrystals and carbon dots on reduced graphene oxide: ternary nanocomposites for accelerated photocatalytic water disinfection, Applied Catalysis B-Environmental, 202 (2017) 33–41. https://doi.org/10.1016/j.apcatb.2016.09.014

Zhang Y.D., Zhang X., Zhao Y.Q., Zhang X.Y., Ding X.K., Ding X.J., Yu B.R., Duan S., Xu F.J., Self-adaptive antibacterial surfaces with bacterium-triggered antifouling-bactericidal switching properties, Biomaterials Science, 8 (2020) 997–1006. https://doi.org/10.1039/c9bm01666j

Zhang Y.Y., Yuan S., Feng X., Li H.W., Zhou J.W., Wang B., Preparation of nanofibrous metal-organic framework filters for efficient air pollution control, Journal of the American Chemical Society, 138 (2016) 5785–5788. https://doi.org/10.1021/jacs.6b02553

Zhao Y.X., Cai W., Chen J.X., Miao Y.Y., Bu Y.F., A highly efficient composite catalyst constructed from NH_2-MIL-125(Ti) and reduced graphene oxide for CO_2 photoreduction, Frontiers in Chemistry, 7 (2019) 789. https://doi.org/10.3389/fchem.2019.00789

Zhou J.L., Hu Z.X., Zabihi F., Chen Z.G., Zhu M.F., Progress and perspective of antiviral protective material, Advanced Fiber Materials, 2 (2020) 123–139. https://doi.org/10.1007/s42765-020-00047-7

Zhu Z., Bao L., Pestov D., Xu P., Wang W.N., Cellular-level insight into biointerface: from surface charge modulation to boosted photocatalytic oxidative disinfection, Chemical Engineering Journal, 453 (2023) 139956. https://doi.org/10.1016/j.cej.2022.139956

Zhu Z., Zhang Y., Bao L., Chen J.P., Duan S., Chen S.C., Xu P., Wang W.N., Self-decontaminating nanofibrous filters for efficient particulate matter removal and airborne bacteria inactivation, Environmental Science: Nano, 8 (2021) 1081–1095. https://doi.org/10.1039/d0en01230k

Authors' Short Biographies

Mohaiminul Haider Chowdhury has been pursuing his Ph.D. in the Department of Mechanical and Nuclear Engineering at Virginia Commonwealth University, USA, under the guidance of Prof. Wei-Ning Wang since Spring 2024. He earned his Master's degree in Renewable Energy Technology from the University of Dhaka, Bangladesh in 2019. His research focuses on the innovative design of efficient photocatalysts for energy- and environmental-sustainable applications.

Dr. Zan Zhu obtained his Ph.D. from the Department of Mechanical and Nuclear Engineering at Virginia Commonwealth University, USA, under the guidance of Prof. Wei-Ning Wang in 2022. He received his Master's degree in Optical Engineering from the Beijing Institute of Technology in 2016. His research at VCU focused on the design of metal-organic frameworks (MOFs)-based functional materials for better air quality.

Prof. Wei-Ning Wang is an Associate Professor in the Department of Mechanical and Nuclear Engineering at Virginia Commonwealth University. He received a Ph.D. degree in Chemistry and Chemical Engineering from Hiroshima University in 2006 and worked as a JSPS postdoctoral fellow from 2006 to 2007. He served as an Assistant Professor at Hiroshima University from 2007 to 2009. He was a Postdoctoral Research Associate at Washington University in St. Louis from 2009 to 2012 and served as a Research Assistant Professor from 2013 to 2014. His research interests include functional material design, synthesis, and characterization, as well as their applications to address energy and environmental issues.